EPJ Web of Conferences **282**, 01007 (2023) https://doi.org/10.1051/epjconf/202328201007
SSP 2022

Chiral symmetry breaking: Current experimental status and prospects

Jan Friedrich[1,*]
on behalf of the COMPASS Collaboration

[1]Physik-Department, Technical University of Munich

Abstract. Chiral symmetry, linked to the smallness of the quark masses compared to the QCD bound states, and its breaking pattern are exploited in effective field theory to describe a multitude of phenomena by a few low-energy constants. Those concern light-meson dynamics and decays, their couplings to photons and meson-nucleon interactions. Special emphasis is given to the pion properties, in terms of pion-pion low-energy scattering, the pion polarizability and the chiral anomaly, which describes the coupling of three pions to a photon. These properties are studied by the COMPASS collaboration at CERN since first data taking with pion beams in the year 2004, and several following campaigns. In the framework of the upcoming AMBER collaboration, it is planned to extend the studies to the kaon sector.

1 Introduction

Exploring the limit of vanishing masses in quark fields of the Lagrangian of Quantum Chromodynamics (QCD),

$$\mathcal{L}_{QCD} = \overline{\psi}_q \left(i\gamma^\mu(\partial_\mu + igA_\mu) - m_q \right) \psi^q \quad (1)$$

it turns out that left- and right-handed quarks, q_L and q_R respectively, decouple and $\mathcal{L}_{QCD}$ is chirally symmetric for $m_q \to 0$. The index q denotes the different quark flavors $u, d, s, ...$, color indices are suppressed. This symmetry is broken explicitly by the small but non-zero quark masses, but also spontaneously in the sense that the physical vacuum does not feature the symmetry. Assuming the symmetry breaking to be a small variation, a systematic expansion of QCD at low momenta can be formulated, known as Chiral Perturbation Theory (ChPT). Pions play a central role as the (approximate) Goldstone bosons related to the chiral symmetry, and the measurement of their properties and dynamics allow to test the assumptions made in the theoretical framework, which had been pioneered by Weinberg and Goldstone, and later worked out by others [1–4]. Since ChPT is a low-momentum expansion, it converges fastest for small relative particle momenta, and at higher momenta the range of validity is constrained by higher orders within the theory, which are only calculated up to a certain order, and by the contribution of resonances, which are not included in the framework of ChPT. The domain where ChPT is relevant for the measurement depends on the concerned

*e-mail: jan@tum.de

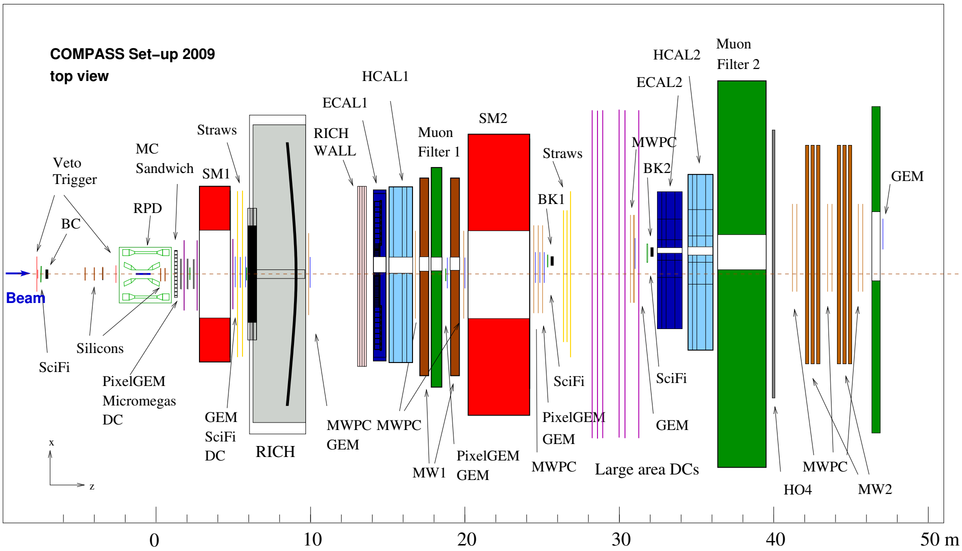

Figure 1. Layout of the COMPASS setup as used for hadron beams in the years 2008 and 2009. A detailed description of the employed detectors can be found in [7]. The spectrometer magnets SM1 and SM2, equipped up- and downstream with tracking detectors and followed by calorimeters, constitute the two stages of the setup.

process, but in general there is a range from the kinematic threshold of the process up collision energies where resonances become relevant – typically a few pion masses – where ChPT is expected to explain the dominant part of the cross sections.

The pion-pion interaction was studied by the NA48/2 Collaboration at the CERN SPS in Kaon decays, where the final-state interaction is sensitive to the pion scattering length [5], and by the E865 experiment at BNL [6].

2 Measurements at COMPASS

The COMPASS experiment uses secondary hadron and tertiary muon beams from the CERN 450 GeV super proton synchrotron (SPS). The multi-purpose detector concept allows for a wide range of investigations in hadron physics, with high-precision and high-rate capable tracking, particle identification and calorimetry in both stages of the magnetic spectrometer. The layout of the setup is shown in Fig. 1. The two stages are optimized for low and high momentum particles, respectively, and allow a momentum determination of better than 1% in a wide range, from about 1 GeV up to the beam momentum in the range of 200 GeV.

The method used to study pion-photon reactions is attributed to H. Primakoff [8]. It makes use of the intense electric field in the proximity of nuclei, which can be treated in a high-relativistic reference system as a source of quasi-real photons, to study strongly-interacting particles. The original idea concerned the measurement of the π^0 lifetime by photon-photon fusion, but it was later realized that interactions by high-energetic hadrons with the nuclear Coulomb field represent similarly a scattering off the quasi-real photon density, and consequently the whole set of such hadron interactions is referred to as Primakoff reactions.

2.1 Chiral dynamics in $\pi\gamma \to 3\pi$

An early analysis of COMPASS using the Primakoff technique was completed for the reaction $\pi^-\gamma \to \pi^-\pi^-\pi^+$ [7], of data from a pilot run in the year 2004. The region with 3-pion masses below 1 GeV is of specific interest in terms of chiral dynamics: The tails of known resonances play only a minor role, and the relative pion momenta are small, such that the kinematics lies in the region where ChPT is applicable. ChPT provides predictions for the absolute cross section to leading [9] and next-to-leading [10] order. In order to compare on the absolute level, a flux normalization for the data had to be done. For the purpose, the kaon component of the hadron beam was used, since some of the kaons decay in the free space around the target with well-known branching into the same three-pion final state as under study here, also with practically vanishing momentum transfer. Taking into account the kaon-to-pion fraction in the beam, the effective flux of pions is deduced from the number of observed kaon decays. Measuring the same final state, it features a similar reconstruction efficiency, that has to be propagated to the full mass spectrum of interest only moderately by the Monte Carlo simulation of the setup.

The result for the cross section of $\pi^-\gamma \to \pi^-\pi^-\pi^+$ is published in [11]. The absolute cross-section has been determined in five bins of the final-state mass from threshold at $3m_\pi$ up to $5m_\pi$. The data agree with the expectation from tree-level ChPT on the level of the experimental uncertainty of 20%. This confirms the extension of the ChPT approach for processes involving the coupling of four pions, *i.e.* the leading order, to processes involving the additional coupling to a photon. In terms of studying ChPT, the neutral channel $\pi^-\gamma \to \pi^-\pi^0\pi^0$ will be of even higher relevance, since for this channel higher-order loop corrections are expected to play a large role [10].

2.2 Measurement of the pion polarisability

The measurement of the pion polarisability has been one of the genuine goals in the proposal of the COMPASS experiment. After the pilot run in the year 2004, data have been collected in a two-week beam time in 2009 with significant improvements concerning the calorimetry and the trigger system, as concluded from the detailed analysis of the 2004 data. It was also found [12] that lead is not a favorable target material despite the high nuclear charge Z, since the radiative corrections due to multiple photon exchange and screening are large and represent a non-negligible source of systematic uncertainty. Consequently, the measurement was performed with a 4 mm thick nickel disk as nuclear target.

A unique feature of the pion polarisability measurement at COMPASS is that the beam can be switched, within less than an hour, from hadron to muon beam, and the spectrometer is well equipped for muon identification due to the broad physics program with muon beams. For the polarisability measurement, this allows for control measurements with muon beam, for which the theoretical expectation of the relevant bremsstrahlung process μ^- Ni$\to$ $\mu^-\gamma$ Ni is completely determined by quantum electrodynamics (QED).

The result has been published in [13], $\alpha_\pi = (2.0 \pm 0.6_{stat} \pm 0.7_{syst}) \cdot 10^{-4}$ fm^3. Radiative corrections have been applied on the level of the simulation event-wise, starting from the published calculations [14, 15] for the case of pion and muon Compton scattering, respectively, and extrapolating to the Primakoff kinematics at $Q^2 \neq 0$. Detailed information about the analysis of these data can be found in [16] The presented preliminary COMPASS value for the pion polarisability is at variance from the historically first result obtained at Serpukhov [17], also employing the Primakoff technique, which had been confirmed much later by the dedicated experiment on radiative pion photoproduction at MAMI [18]. In the mean time, the available data on $\gamma\gamma \to \pi^+\pi^-$ at e^-e^+-colliders were re-interpreted by several authors [19–22] claiming very different values for the pion polarisability. Later on, it had been proven that there is no conflict between ChPT and dispersion theory [23, 24].

So, the COMPASS result is in significant tension with the earlier experimental determinations of the pion polarisability, but it is in good agreement with the expectation of chiral perturbation theory [25].

3 Analysis of the Chiral Anomaly

The chiral anomaly constant

$$F_{3\pi} = \frac{eN_C}{12\pi^2 F_\pi^3} = (9.78 \pm 0.05)\ \text{GeV}^{-3} \tag{2}$$

describes the direct coupling of photons to three pions, as depicted in Fig. 2. In the experiment, it is accessible through the Primakoff reaction embedding $\pi^-\gamma \to \pi^-\pi^0$. The first mea-

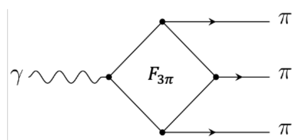

Figure 2. Coupling of a photon to three pions.

surement of $F_{3\pi}$ has been approached in the same Serpukhov experiments as mentioned above in the context of the pion polarisability. In [26], the value $F_{3\pi}^{Serp,orig} = (12.9 \pm 0.9 \pm 0.5)\ \text{GeV}^{-3}$ has been found. Later on, it was realized that a reanalysis is required due to an electromagnetic correction [27], leading to $F_{3\pi}^{Serp,corr} = (10.7 \pm 1.2)\ \text{GeV}^{-3}$. This value is in coarse agreement with the theoretical expectation, but a more precise experimental determination is highly demanded.

Theoretical framework for the analysis of the COMPASS data is the dispersive approach worked out in [28], which extends the useful kinematic range from the chiral low-momentum region beyond the ρ resonance.

The luminosity determination, which is of key importance for this analysis, has been done in principle as described above for the 3-pion data, but now extended to all relevant decay channels of the Kaons. Details of the analysis will be found in the ongoing PhD theses [29]. The preliminary value is $L_{eff} = 5.21 \pm 0.48_{syst} \pm 0.04_{stat}$, where further studies are expected to still reduce the systematic uncertainty. The level of accuracy in decribing the data by the Monte-Carlo simulation is depicted in Figs. 3 and 4 for the Kaon decays.

The most challenging part of the analysis is to control the background to the $\pi^-\gamma \to \pi^-\pi^0$ channel, which stems from reactions $\pi^-\text{Ni} \to \text{Ni}\pi^-\pi^0\pi^0$. They can proceed via Pomeron exchange and thus come with a much larger cross-section, so that even a small fraction, in which the second π^0 remains undetected and accidentally the resulting momentum transfer turns out very small, can become significant in the Primakoff region.

In order to address this background, a full analysis of $\pi^-\text{Ni} \to \text{Ni}\pi^-\pi^0\pi^0$ events is performed, and a partial-wave model fitted to the data. This model can be used as input to the Monte-Carlo simulation, extending the kinematic range into the relevant part, in which the full final state can not be detected, e.g. due to one of the π^0 having an energy too small to be reconstructed. This model can predict the amount of background differential in all kinematic quantities and thus be used to subtract the background with high accuracy. The distribution of the momentum transfer Q^2 for different 2π-mass bins is shown in Fig. 5.

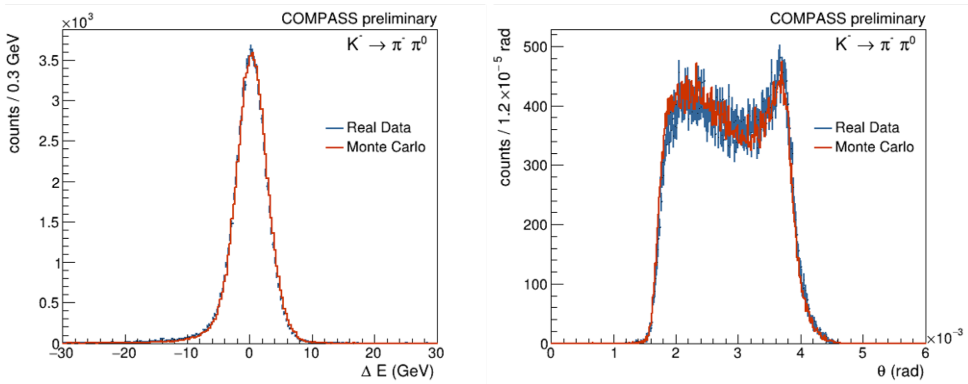

Figure 3. Comparison of the final-state laboratory energy of the Kaon decay products $\pi^-\pi^0$, minus the beam energy (left), and the angular distribution of the outgoing pions (right) with the Monte-Carlo description.

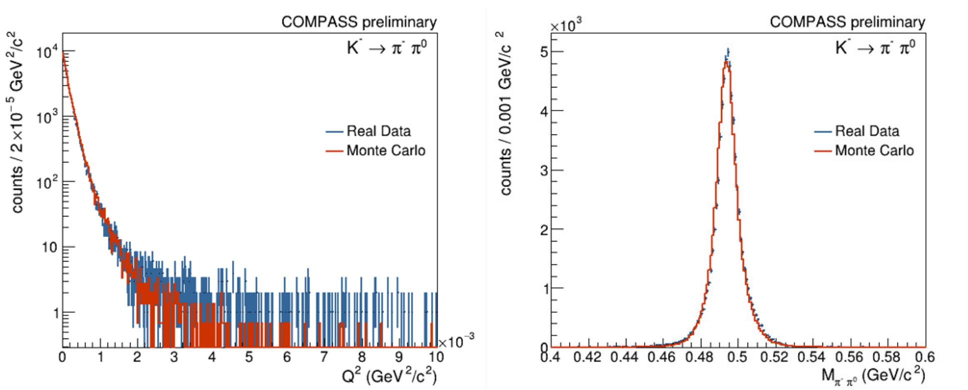

Figure 4. Comparison of the momentum balance in the Kaon decay, reconstructing a hypothetical momentum transfer, which should be zero for infinitely high detector resolution (right), and the invariant mass of the two-pion final-state system (right), with the Monte-Carlo description.

The background has a different shape than the real-data distributions, lacking the prominent Primakoff peak at small Q^2. At larger Q^2, however, it proves to be the dominant part of the distribution. In total, a consistent description of data can be achieved, thus the signal strength determined with high precision. This part of the analysis is currently still being refined.

With the preliminary background subtraction, the two-pion mass distribution shown in Fig. 6 is obtained. We conclude from fitting the model of [28] the value

$$F_{3\pi}^{COMPASS,prelim.} = (10.3 \pm 0.1_{stat} \pm 0.6_{syst}^{prelim.})\ \mathrm{GeV}^{-3} \tag{3}$$

The result confirms the prediction of ChPT, cf. Eq. 2, with a somewhat smaller uncertainty then the earlier experiment at Serpukhov [26]. However, we aim at still significantly reducing the systematic uncertainty. Also, the QED radiative corrections, which have been worked out already, still have to be applied.

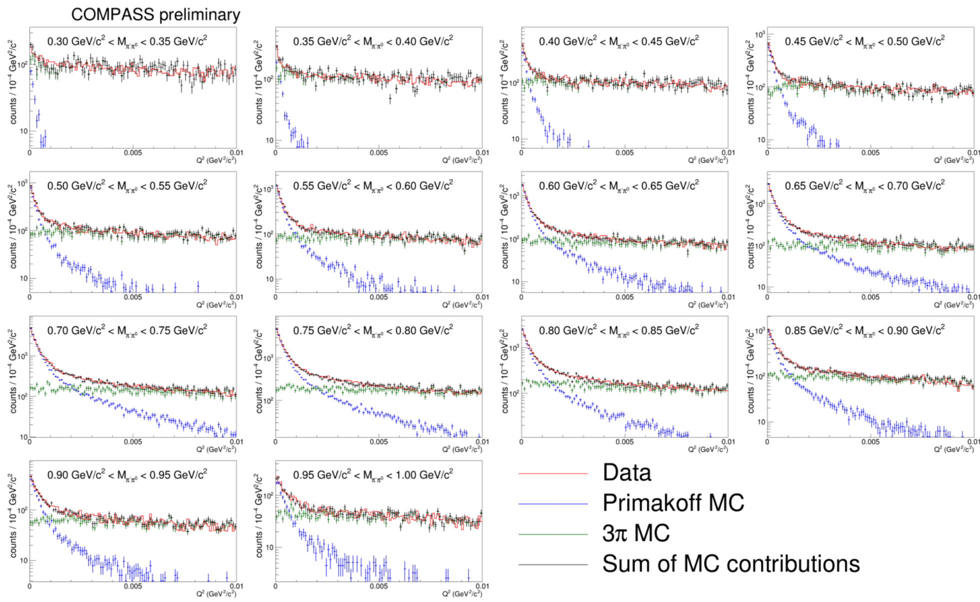

Figure 5. Three-pion background to the two-pion final states for different two-pion mass bins.

Along with analysing the data to extract $F_{3\pi}$, also the higher two-pion masses are investigated. In fact, the dispersive approach of [28] suggests to fit at the same time the contribution of the ρ resonance, and extending the two-pion mass window to above 1 GeV as shown in Fig. 6. Since the same production mechanism is at work, the reaction $\pi^-\gamma \to \rho^- \to \pi^-\pi^0$ is determined by the radiative coupling of the ρ. From the same fit that gave the result in Eq. 4, the value

$$\Gamma^{COMPASS,prelim.}_{\rho\to\pi\gamma} = (76 \pm 1_{stat}{}^{+10}_{-8,syst})\ \text{keV} \tag{4}$$

is obtained. It is higher than the value (68 ± 7) keV, given in the PDG tables [30], but somewhat lower than the value (81 ± 4 ± 4) keV, obtained previously with a similar experimental method [31], however apparently neglecting the chiral contribution.

4 Conclusions and Outlook

In summary, COMPASS has contributed in several ways to test the predictions made by chiral perturbation theory as effective low-energy description of QCD. This concerns, first of all, the pion polarisability and the $\pi\gamma \to 3\pi$ transitions. Recently the analysis has been extended to the chiral anomaly $F_{3\pi}$ governing the $\pi\gamma \to 2\pi$ transition at small energies. A preliminary result has been obtained, but the investigations are ongoing especially to reduce the systematic uncertainty. The same analysis allows for a new determination of the radiative coupling of the ρ resonance.

All tests done so far with COMPASS data have confirmed the predictions of ChPT. For further challenging the theory, more precise tests are needed. COMPASS has taken more data in the year 2012, which can be analysed in the same spirit as the data from 2009, that have been shown in detail here.

On the longer range, similar studies are planned using the kaon beam component with the successor experiment of COMPASS, having been approved by the CERN SPS committee as

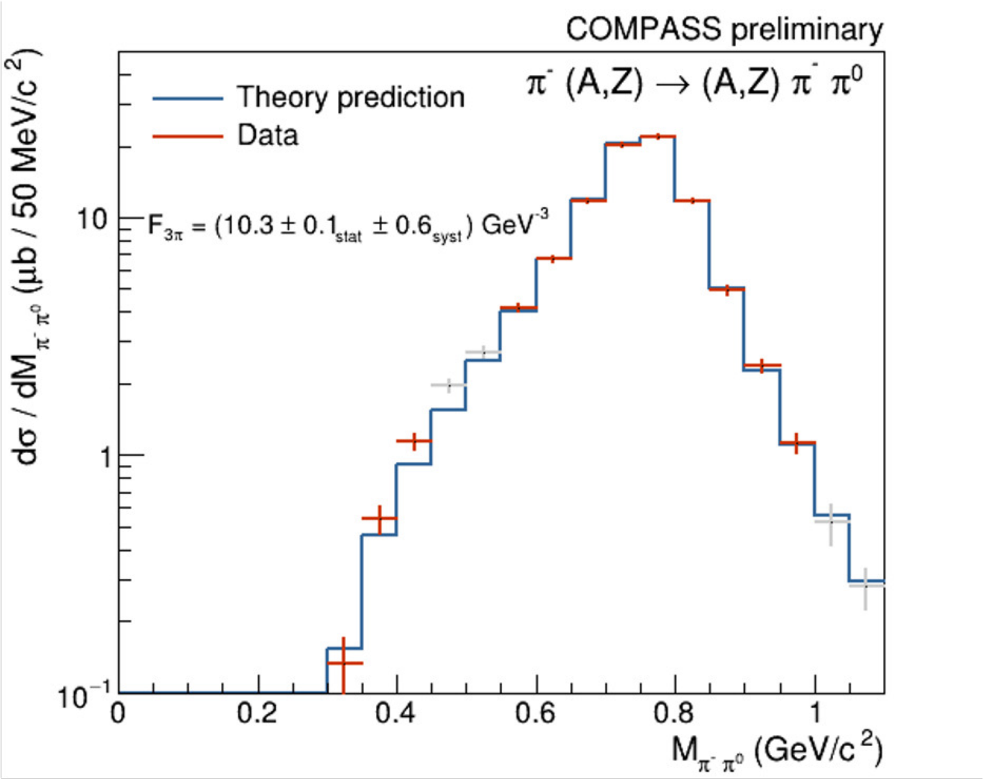

Figure 6. The preliminary COMPASS result for the measurement of the cross section of the process $\pi\gamma \rightarrow \pi\pi$, in bins of the invariant mass. The background is subtracted as explained in the text. The data are drawn in red points with their total uncertainties. The fit of the used theory framework is indicated as blue line. The region affected by decay of beam Kaons into the same final state is excluded in the fit, the respective data points shown in grey.

NA66/AMBER [32] for its Phase-1. Primakoff reactions with kaons are considered in Phase-2, and the theoretical base has recently been worked out [33] for the channel analogous to the chiral anomaly described for pions above. On the experiment side, enhancements in the beam line shall increase the number of available kaons and allow a better beam particle identification.

References

[1] J. Gasser and H. Leutwyler, Phys. Rep. **87**, 77 (1982).
[2] J. Goldstone, Nuovo Cimento **19**, 154 (1961).
[3] J. Goldstone, A. Salam and S. Weinberg, Phys. Rev. **127**, 965 (1962).
[4] S. Weinberg, Phys. Rev. Lett. **17**, 616 (1966).
[5] N. Cabibbo, Phys. Rev. Lett. **93**, 121801 (2004).
[6] S. Pislak *et al.*, Phys. Rev. D **67**, 072004 (2003), Phys. Rev. D **81**, 119903 (2010).
[7] S. Grabmüller, PhD thesis, Tech. Univ. München (2012), CERN-THESIS-2012-170.
[8] H. Primakoff, Phys. Rev. **81**, 899 (1951).
[9] N. Kaiser and J. M. Friedrich, Eur. Phys. J. A **36**, 181 (2008).

[10] N. Kaiser, Nucl. Phys. A **848**, 198 (2010).
[11] C. Adolph *et al.* [COMPASS Collaboration], Phys. Rev. Lett. **108**, 192001 (2012).
[12] N. Kaiser and J. M. Friedrich, Eur. Phys. J. A **39**, 71 (2009).
[13] C. Adolph *et al.* [COMPASS Collaboration], Phys. Rev. Lett. **114**, 062002 (2015).
[14] N. Kaiser and J. M. Friedrich, Nucl. Phys. A **812**, 186 (2008).
[15] N. Kaiser, Nucl. Phys. A **837**, 87 (2010).
[16] T. Nagel, PhD thesis, Tech. Univ. München (2012), CERN-THESIS-2012-138, http://cds.cern.ch/record/1484476.
[17] Yu. M. Antipov *et al.*, Phys. Lett. B **121**, 445 (1983).
[18] J. Ahrens *et al.*, Eur. Phys. J. A **23**, 113 (2005).
[19] D. Babusci *et al.*, Phys. Lett. B **277**, 158 (1992).
[20] J. F. Donoghue and B. R. Holstein Phys. Rev. D **48**, 137 (1993).
[21] A. E. Kaloshin and V. V. Serebryakov, Z. Phys. C **64**, 689 (1994).
[22] L. V. Fil'kov and V. L. Kashevarov, Phys. Rev. C **73**, 035210 (2006).
[23] B. Pasquini, D. Drechsel and S. Scherer, PoS of "Chiral Dynamics 09", Bern, 037 (2009).
[24] B. Pasquini, D. Drechsel and S. Scherer, Phys. Rev. C **81**, 029802 (2010).
[25] J. Gasser, M. A. Ivanov and M. E. Sainio, Nucl. Phys. B **745**, 84 (2006).
[26] Yu. M. Antipov *et al.*, Phys. Rev. D **36**, 101103 (1987).
[27] L. Ametller *et al.*, Phys. Rev. D **64**, 094009 (2001).
[28] M. Hoferichter, B. Kubis, D. Sakkas, Phys. Rev. D **86**, 116006 (2012).
[29] PhD theses of D. Ecker and A. Maltsev, in preparation.
[30] P.A. Zyla *et al.* (Particle Data Group), Prog. Theor. Exp. Phys. 2020, 083C01 (2020).
[31] L. Capraro *et al.*, Nucl. Phys. B **288**, 659 (1987).
[32] B. Adams *et al.*, AMBER Proposal, CERN-SPSC-2019-022; SPSC-P-360, http://cds.cern.ch/record/2676885.
[33] M. Dax, D. Stamen, B. Kubis, Eur. Phys. J. C **81**, 221 (2021).